DYNAMIC STATE OF RIVER-MOUTH BAR IN YURAGAWA RIVER AND APPLICATION OF DRONE PHOTOGRAPHY IMAGE TO OBTAIN ITS TOPOGRAPHIAL DATA

HIROSHI MIWA
Department of Social Systems and Civil Engineering, Tottori University, Tottori, Japan, miwa-h@tottori-u.ac.jp

MIO OMURA
Department of Engineering Design, WESCO Co., Ltd., Okayama, Japan, m-omura@wesco.co.jp

TAKASHI WADA
Department of Social Systems and Civil Engineering, Tottori University, Tottori, Japan, wada-t@tottori-u.ac.jp

YOSHINORI KATO
Department of Civil Engineering and Architecture, National Institute of Technology, Maizuru College, Maizuru, Japan, kato@maizuru-ct.ac.jp

KEIICHI KANDA
Department of Civil Engineering, National Institute of Technology, Akashi College, Akashi, Japan, kanda@akashi.jp

ABSTRACT

Topographic changes of the river-mouth bar in the Yuragawa River of Japan are continuously activated by sediment transport due to river flows and sea waves. A large part of the bar was eroded by the flood flow due to Typhoon No.23 in October 2004. The bar has formed on the right bank only since then. The size of the bar has gradually decreased as a long-term tendency, whereas the expansion of the bar due to transportation of drift sand into the estuary has been identified in recent years. These situations may cause problems such as washout of bank protection works, intrusion of drift sand into irrigation canals. In order to clarify the characteristics of the topographical changes of the bar and their causes, we need to analyze the temporal variations in geometrical properties of the bar on the basis of the topographical and hydrological data in the estuary. The topographical data have often been obtained by using a RTK-GNSS receiver, which can show high precision and accuracy. However, this method may have disadvantage for swift actions upon a disaster investigation. In recent years, an aerial photography image can be easily taken by a drone. We propose a method of introducing the images and a coordinate transformation into obtaining shoreline data, and then compare the obtained results with the RTK-GNSS data. The DRMS values concerning with the coordinate values of GCPs were approximately a few meters in maximum. As for the area of the river-mouth bar, the estimation results based on the proposed method kept an error within a few percent, the large-scale variations in the area due to large flood could also be grasped.

Keywords: River-mouth bar, topographical change, drone, combined image, affine transformation

1. INTRODUCTION

A river-mouth is defined as a region where river runoff enters an ocean, its topography is characterized by the combined influences of sediments transported by river flows and near shore currents associated with tides and sea waves. River-mouths along the Sea of Japan are particularly affected by winter sea waves and tidal prisms are relatively small. Therefore, river-mouth bars tend to develop by the coastal sand drift, and the river mouth blocking has occurred frequently. The bars developed in the dry season tend to be flushed out by floods in the summer and rainy season, and bar behavior during floods and river-mouth channel width after flushing the bars changes complexly. These changes vary depending on flood discharges, river-mouth topography and the presence or absence of harbor facilities and other man-made structures along the coast.

The Yuragawa River located in the north of Kyoto Prefecture (Figure 1) has a length of 146 km and a basin area of 1,880 km^2, and its system is one of the 109 Class A river systems in Japan. Topographic changes of its river-mouth bar have been continuously activated by sediment transport due to river flows and sea waves. In October 2004, a large part of the river-mouth bar was eroded by the flood flow of Typhoon No.23. Since then, the river-mouth bar has developed on the right bank only as shown in Figure 2, and the river-mouth channel has been fixed along the left bank. This situation may cause some problems such as bank erosion, washout of bank protection works and harmful effects on other coastal structures. In order to avoid these problems and risk, it is important to understand the characteristics of the topographic change of the river-mouth bar and their cause,

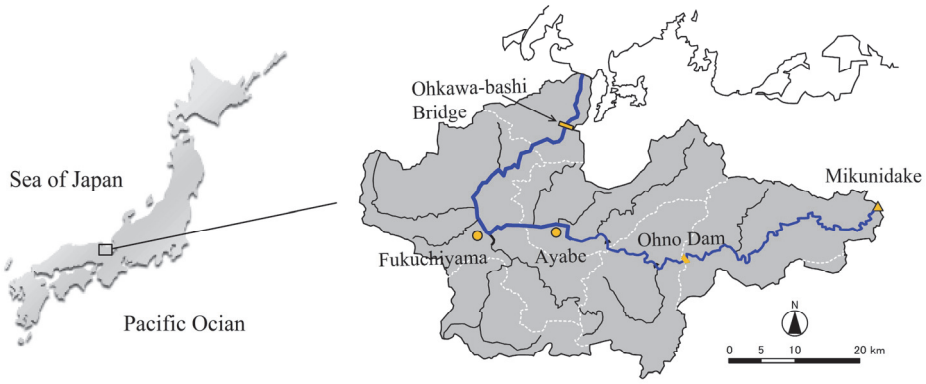

Figure 1. Location and basin of the Yuragawa River.

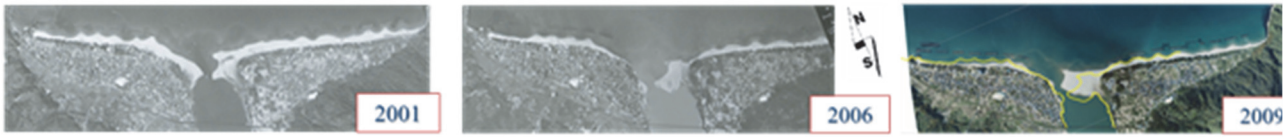

Figure 2. Topographic changes in river-mouth topography in the Yuragawa River before and after flood in 2004.

and to propose a control method of the bar geometry. Ochi et al. (2015) investigated the temporal variations in the area of the river-mouth bar for almost four years from May 2010. Then they found that the area of the bar increased and decreased in the short-term, and also investigated the effects of the water discharges due to floods and wave heights in winter seasons on the area of the bar. Nakamura et al. (2015) carried out the numerical simulation for the developing process of the river-mouth bar using the field measurements for the bar and sea wave. As a result, they clarified that the development of the river-mouth bar is caused by the transportation of the sediment in the sea by the wave. Miwa et al. (2016) investigated the effectiveness of a trench excavation and a spur dike, which can increase the erosion area of the bar and change of the flow direction respectively, in order to control the river-mouth bar by the flume experiments and numerical simulations. They also reported that the area of the river-mouth bar had gradually decreased in the long-term basis. However, the situation of that in recent years has unknown.

The field surveys in the research mentioned above carried out by using a GNSS receiver with RTK (Realtime Kinematic) system (RTK-GNSS receiver), which can show high precision and accuracy. Ministry of Land, Infrastructure, Transport and Tourism (2020) of Japan has promoted an application of ICT (Information and Communication Technology) to construction sites in recent years. In particular, 3D survey using a drone, or a laser scanner has played an important role in many construction sites. However, this apparatus has disadvantage for swift actions upon occurring a flood disaster, and its restricted access. It also needs a relatively long-time for carrying out the field survey. In recent years, a drone has been applied in several fields, and the field surveys in civil engineering because an aerial photography image can be easily taken by using a drone with a high-resolution camera. Obanawa et al. (2014) compared UAV-based SfM (Structure from Motion) data against TLS (Terrestrial Laser Scanning) derived DSM (Digital Surface Model) data. The fieldwork was carried out on a wave-cut bench in Kanagawa Prefecture, Japan. Results have indicated that DSM data derived from UAV-SfM can create a point cloud of comparable density to the one created by TLS, with a maximum deviation of 10 cm from the TLS data. Tanaka et al. (2016) proposed the method of topographical survey by using the aerial motion video, and they applied it to the debris flow disaster site. Kuroiwa et al. (2016) analyzed the coastal topographic change in the Uradome beach in Tottori Prefecture in Japan on the basis of the three-dimensional model using SfM associated with the aerial images obtained by a drone. As a result, the observation along the coastline worked out in 20 minutes about 2 kilometers. The accuracy of the observation between the RTK-GPS and the drone survey was 0.05 m of RMSE value. Kawaguchi et al. (2019) conducted the RTK-GNSS survey in the disaster area, where had a damage by high waves and a high-tide due to a typhoon in 2017. They spatially estimated the detailed inundation height and depth by using the photography images. In these studies, results of comparatively high accuracy were obtained by introducing a SfM software into the analyses. However, the exact precision and accuracy are not always required when we want to understand the dynamics of the river-mouth bar. Therefore, a simpler method may be considered.

In this study, temporal variations in geometrical properties (e.g. area) of the river-mouth bar were analyzed on the basis of the hydrological and topographical data in the Yuragawa River estuary. The effects of the river water discharge and the sea wave height on the geometrical properties of the bar were investigated. The situation of the river-mouth bar in recent years was also discussed. As for the measurement of the shoreline, we proposed the method of calculating coordinate values of stations on the shoreline by a coordinate transformation using

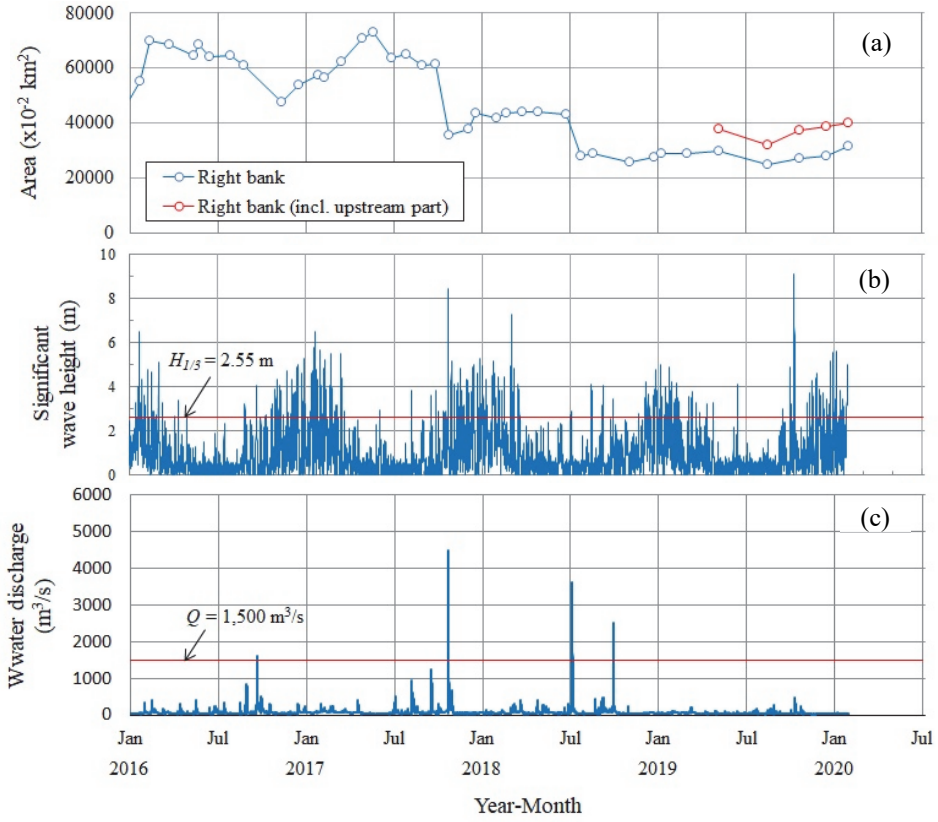

Figure 3. Temporal variations in (a) river-mouth bar area, (b) significant wave height at Kyoga-Misaki, and (c) water discharge at Fukuchiyama in the Yuragawa River.

aerial photography images by a drone and grand control points (GCPs). This method applied to not only the Yuragawa river-mouth zone but also the Kanzaki coastal zone which is located at the east side of the Yuragawa river-mouth. The calculated results of their shorelines were compared with the measurement results by the RTK-GNSS survey. The estimation results of the areas of these zones by using the calculated results of the shorelines were also compared with those by using the measurement results of the shorelines, and then effectiveness of the proposed method was discussed.

2. FIELD MEASUREMENTS ON RIVER MOUTH TOPOGRAPY

In order to clarify the effects of river flow discharge and sea wave height on changes in river-mouth topography after 2016, survey works were conducted by using RTK-GNSS receiver (GRX1, Sokkia Topcon Co., Ltd.) periodically. A surveyor walked along the shoreline receiving the satellite signals, and registered the signal to the controller at intervals of approximately 15 to 20 m. The number of stations for each survey was about 70 to 100. The survey was basically conducted once every one or two months. The shape and area of the bar were calculated from the measured coordinates of the stations. There were no corrections of the sea level relates to a tide level because the tidal range is at most 30 cm, which may not affect the shoreline significantly.

Figure 3 shows the temporal variations in the area of the river-mouth bar, the significant wave height at Kyoga-Misaki (30 km away from the river-mouth) and the water discharge at Fukuchiyama (37 km away from the river-mouth) for about four years (from January 2016 to January 2020). The area of the river-mouth bar kept on fluctuating until July 2018, whereas the fluctuation is not so large after that. As concerns of the short-term tendency, the area increased in the winter seasons of 2016, 2017 and 2018, and it decreased in their summer and rainy season. Kanda et al. (2012) clarified that the significant wave height over 2.55 m influences the development of the river-mouth bar. As shown in Figure 2(b), such high significant wave heights were observed in the winter season. Therefore, it would be considered that an increase in the onshore sediment transport in the winter season may contribute to the development of the river-mouth bar. A possible reason why the area hardly increases in the winter seasons of 2019 and 2020 is that the drift sand from the offshore may be accumulated on the seabed eroded by the flood flow on July and September 2018. Kanda et al. (2012) also clarified that the water discharge over 1,500 m^3/s affects the area of the river-mouth bar. As shown in Figure 3(c), the water discharge over 1,500 m^3/s was recorded a total of four times in this observation period. In particular, the flood with discharge of about 4,500 m^3/s occurred due to Typhoon No.21 in September 2017. The flood with discharge of about 3600 m^3/s also occurred due to Typhoon No.7 and a seasonal rain front in 2018. These floods reduced the area of the river-mouth bar by approximately 42 % in 2017 and approximately 35 % in 2018.

Most of the river-mouth bar in the Yuragawa River has almost been flushed out by some large floods in recent

years. However, the expansion of the river-mouth bar has been identified at the upstream of the present bar. The red symbols in Figure 3(a) show the area of the river-mouth bar including the upstream bar, which might have been formed since the winter season of 2017-2018. This may be because the drift sand from the offshore has more easily entered to the estuary. Since the river-mouth bar has repeated development and decline on a long-term basis, the filed survey has to be continued. The method obtaining a shoreline by using a drone is developed in the following chapter.

3. TOPOGRAPHIAL DATA BY USING DRONE PHOTPGRAPHY IMAGES

3.1 Aerial photography by drone and arrangement of photographs

The aerial photography was conducted by using a drone (Phantom 4, DJI co., Ltd.). The drone was controlled by the monitoring application DHI Go 4.0. The specifications of the drone are listed in Table 1. The image file format is JPEG and each image file has recorded the longitude, latitude and altitude (ellipsoid height) of the drone which took the image. Since the drone camera was set downward in the vertical direction, the center of the image matches its recorded longitude and latitude. Therefore, the distortion of the image increases as the distance from the center of the image. In order to reduce the distortion of the image, the subjects were photographed overlapping. We could also take an image file of JPEG format from the aerial motion video. The distortion of the image file was occurred in this method too. Therefore, the image files have to be taken overlapping.

Table 1. Technical specification of drone (Phantom 4).

Item	Value / Type
Weight	1380 g
Diagonal size and height	350 mm, 197 mm (Propeller excluded)
Maximum flight time	Approx. 28 min
Satellite positioning systems	GPS / GLONASS
Maximum transmission distance	5000 m
Maximum speed	20 m/s (Sport mode)
Camera	4K, 30 fps (Video), 4000 x 3000 pixels (Image)

The target area of the aerial photography is the Yuragawa river-mouth zone. We also carried out the aerial photography to the Kanzaki coastal zone which is located at the east side of the river-mouth because we check the applicability of our method to a coastal zone. Since these areas are relatively wide, we divided the areas into three and carried out the photography for each area along the shoreline. The altitude of the drone was kept at 140 m and the motion videos and photographs were taken from there. The flight distance of the drone was within the visual range (approximately 400 m) and some takeoff and landing points were arranged. The photography operation was conducted by two persons of a control pilot and a drone observer. Each operation time was approximately 15 to 20 minutes. Table 2 shows the date of the aerial photography and the record type of the target areas. The situations of the target areas of Run Nos.1 to 4 were recorded in the motion videos, and those still-images were captured from the videos. The situations of the target areas of Run Nos.5 to 7 were recorded as the still-images. The combined images of the target areas are made from these still-images. The examples of the combined images of the Yuragawa river-mouth zone and Kanzaki coastal zone are shown in Figure 4.

Table 2. Date of aerial photography and record type of target zones.

Run No.	Date	Yuragawa river-mouth zone	Kanzaki coastal zone
1	Apr. 28, 2018	Video	—
2	Jun. 26, 2018	Video	—
3	Jul. 26, 2018	Video	Video
4	Aug. 21, 2018	Video	Video
5	Nov. 6, 2018	Photo	Photo
6	Jan. 14, 2019	Photo	Photo
7	Mar. 5, 2019	Photo	Photo

3.2 Coordinate transformation and its accuracy

The coordinate values of stations on the shoreline in the combined image have to be transformed to the plane rectangular coordinate system. We introduced an affine transformation to the coordinate transformation in this study. That is, some GCPs are chosen in the combined images first. The affine transformation coefficients are calculated so that the coordinate values of GCPs in the combined image match their coordinate values in the plane rectangular coordinate system next. And then, the coordinate values of the stations on the shoreline in the combined image are transformed into the coordinate values in the plane rectangular coordinate system using the

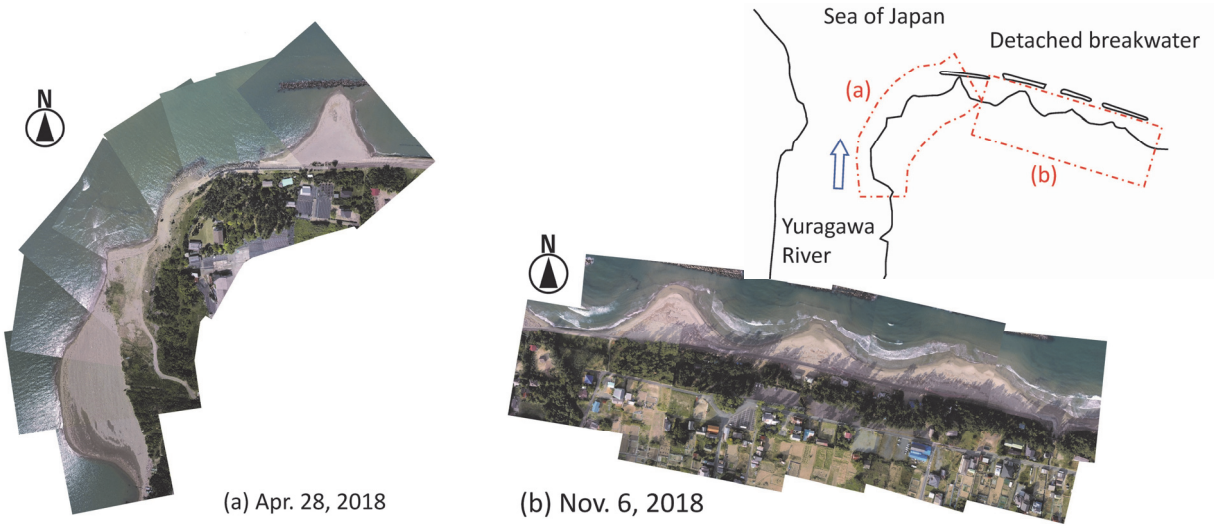

Figure 4. Examples of combined images of Yuragawa river-mouth zone (right bank) and Kanzaki coastal zone.

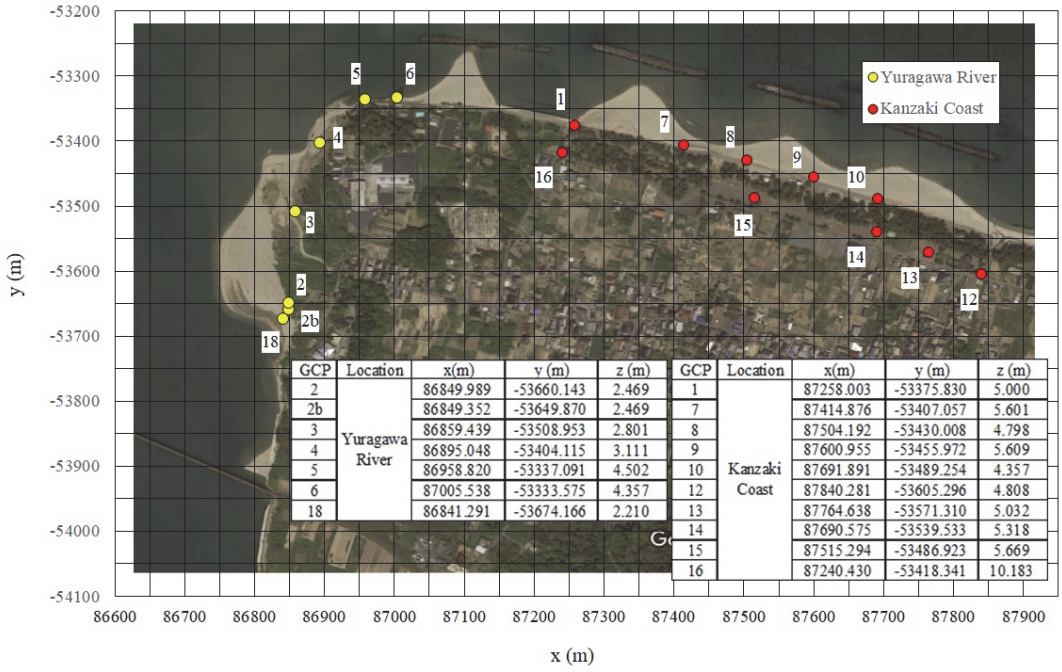

GCP	Location	x(m)	y (m)	z (m)
2	Yuragawa River	86849.989	-53660.143	2.469
2b		86849.352	-53649.870	2.469
3		86859.439	-53508.953	2.801
4		86895.048	-53404.115	3.111
5		86958.820	-53337.091	4.502
6		87005.538	-53333.575	4.357
18		86841.291	-53674.166	2.210

GCP	Location	x(m)	y (m)	z (m)
1	Kanzaki Coast	87258.003	-53375.830	5.000
7		87414.876	-53407.057	5.601
8		87504.192	-53430.008	4.798
9		87600.955	-53455.972	5.609
10		87691.891	-53489.254	4.357
12		87840.281	-53605.296	4.808
13		87764.638	-53571.310	5.032
14		87690.575	-53539.533	5.318
15		87515.294	-53486.923	5.669
16		87240.430	-53418.341	10.183

Figure 5. Grand control point (GCP) in Yuragawa river-mouth zone and Kanzaki coastal zone mounted on the Google image on October. 2018 (2018).

affine transformation coefficients. The coordinate value (U, V) in the combined image is transformed into the coordinate value (X, Y) in the plane rectangular coordinate system by using the following relation:

$$\begin{cases} X = aU + bV + c \\ Y = dU + eV + f \end{cases} \tag{1}$$

where a - f = affine transformation coefficients, which are obtained by the following equations:

$$\begin{pmatrix} a \\ b \\ c \end{pmatrix} = A^{-1}\begin{pmatrix} \Sigma xu \\ \Sigma xv \\ \Sigma x \end{pmatrix}, \quad \begin{pmatrix} d \\ e \\ f \end{pmatrix} = A^{-1}\begin{pmatrix} \Sigma yu \\ \Sigma yv \\ \Sigma y \end{pmatrix}, \quad A = \begin{pmatrix} \Sigma u^2 & \Sigma uv & \Sigma u \\ \Sigma uv & \Sigma v^2 & \Sigma v \\ \Sigma u & \Sigma v & \Sigma 1 \end{pmatrix} \tag{2}$$

where u and v are the lateral and longitudinal coordinate values of the GCP in the combined image, respectively. x and y are those in the plane rectangular coordinate system.

Figure 5 shows the GCPs in the Yuragawa river-mouth zone and Kanzaki coastal zone. The lateral (x) and longitudinal (y) coordinate values of them are listed in the figure. These values are indicated based on Zone V in the plane rectangular coordinate system. The ground level value (z) of the GCP indicates the relative value to the grand level value of GCP No.1, which was given as 5 m in this study. We verify the accuracy of the calculated coordinate values based on the affine transformation by using the combined images and coordinate values of GCPs listed in Figure 5. The station Nos.2, 4 and 6 for the Yuragawa river-mouth zone and station

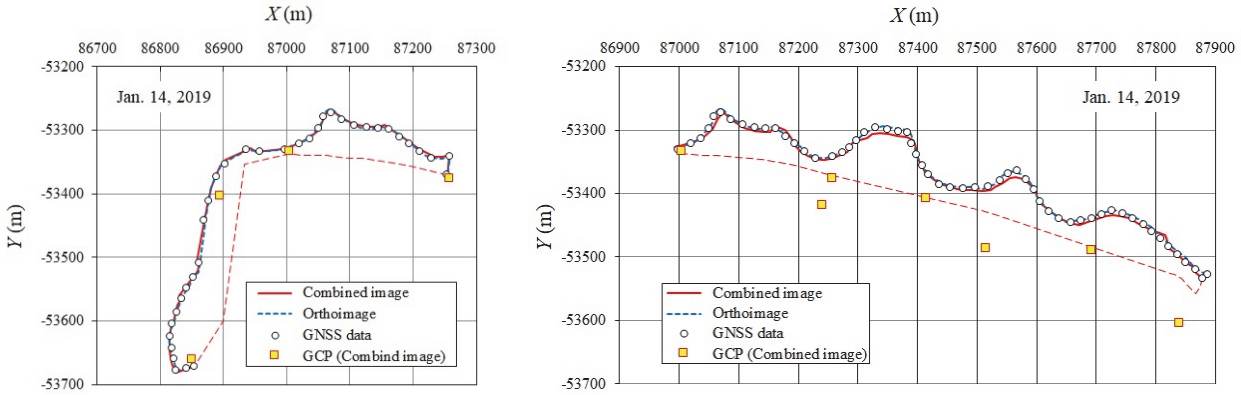

(a) Yuragawa river-mouth zone (b) Kanzaki coastal zone

Figure 6. Examples of estimation and measurement results of shoreline and their comparison.

Nos.1, 8, 12 and 15 for the Kanzaki coastal zone were used as the GCP in the affine transformation. We used the software, Simple Digitizer (Fujimaki, 2011), for taking the coordinate values of the GCPs in the combined images. Table 3 shows the calculated coordinate values of the verification stations (chosen GCPs) and their *DRMS* which is defined as

$$DRMS = \sqrt{\sigma_x^2 + \sigma_y^2}\,, \quad \sigma_x^2 = \frac{1}{n}\sum_{i=1}^{n}(X - x)^2\,, \quad \sigma_y^2 = \frac{1}{n}\sum_{i=1}^{n}(Y - y)^2 \tag{3}$$

Table 3. Calculated coordinate values of verification stations and their *DRMS*

GCP No.	Zone	RTK-GNSS		Combined image					Orthoimage				
		x (m)	*y* (m)	*X* (m)	*Y* (m)	*X-x* (m)	Y-y (m)	*DRMS* (m)	*X* (m)	*Y* (m)	*X-x* (m)	*Y-y* (m)	*DRMS* (m)
3	Yuragawa river-mouth	86859.44	-53508.95	86860.21	-53511.83	0.77	-2.87	2.30	86859.43	-53509.39	0.00	-0.43	0.34
5		86958.82	-53337.09	86956.80	-53337.52	-2.02	-0.43		86958.55	-53336.80	-0.27	0.29	
18		86842.29	-53674.17	86842.95	-53674.28	1.66	-0.11		86841.23	-53674.14	-0.06	0.03	
7	Kanzaki coast	87414.88	-53407.06	87415.59	-53406.66	0.71	0.40	4.18	87415.32	-53407.16	0.44	-0.10	0.58
13		87764.64	-53571.31	87769.99	-53573.23	5.36	-1.92		87764.04	-53571.33	-0.59	-0.02	
16		87240.43	-53418.34	87244.82	-53418.19	4.39	0.15		87239.76	-53418.38	-0.67	-0.04	

The error (*X-x*, *Y-y*) are identified within 3 m for the Yuragawa river-mouth zone, whereas it is identified relatively large for the Kanzaki coastal zone. As a result, *DRMS* value of Kanzaki coastal zone is about twice the larger than that of Yuragawa river-mouth zone. These errors may be caused by the distortion of the image and the personal attributes. However, since the error within 1 m can also be found in the calculated results, a certain degree of accuracy could be secured if the selection of the still-image and combination of them are reasonably. In this study, we also executed the affine transformation using the orthoimages for comparison. The orthoimage was generated by the SfM software (Pix4Dmapper, Pix4D S.A.) using the still-images taken by the drone. The GCPs for the affine transformation were same as the execution for the combined images mentioned above. The calculated results are also listed in Table 3. The errors are identified within 1 m for both zones. This accuracy is equivalent to the accuracy of DGPS (Differential GPS) receiver. The reasonable number of GCP for the calculation of the coordinate value of a station is not so many for using orthoimages, but more GCPs are better for using combined images.

3.3 Estimation of shorelines and areas of Yuragawa river-mouth and Kanzaki coastal zones

We estimated the coordinate values of shorelines in the two zones of the date listed in Table 2 with the method described in the previous chapter using the combined images. The station Nos.1, 2, 4 and 6 for the Yuragawa river-mouth zone and the station Nos.1, 6, 7, 10, 12, 15 and 16 for the Kanzaki coastal zone were used as the GCP in the affine transformation. These GCPs were the same for all field observations. The example of the estimation results of the shorelines in Yuragawa river-mouth zone and Kanzaki coastal zone are shown in Figure 6. The measured results with RTK-GNSS receiver and the locations of GCP are also shown in the figure. The red broken line in the figure shows the border of the river-mouth zone or coastal zone in land. It can be found that the estimation results roughly follow the shorelines measured by the RTK-GNSS surveys in both zones. The relatively low accuracy in Kanzaki coastal zone might be caused by not only the distortion of the image but also the unbalanced arrangement of GCPs. Since the Kanzaki coastal zone extends in the East-West direction, the GCP may have to be set in the North - South direction widely too. The estimation results by using the orthoimage are shown in the figure for comparison. The station Nos.5, 13, 15 and 18 (No.2 for only Nov. in

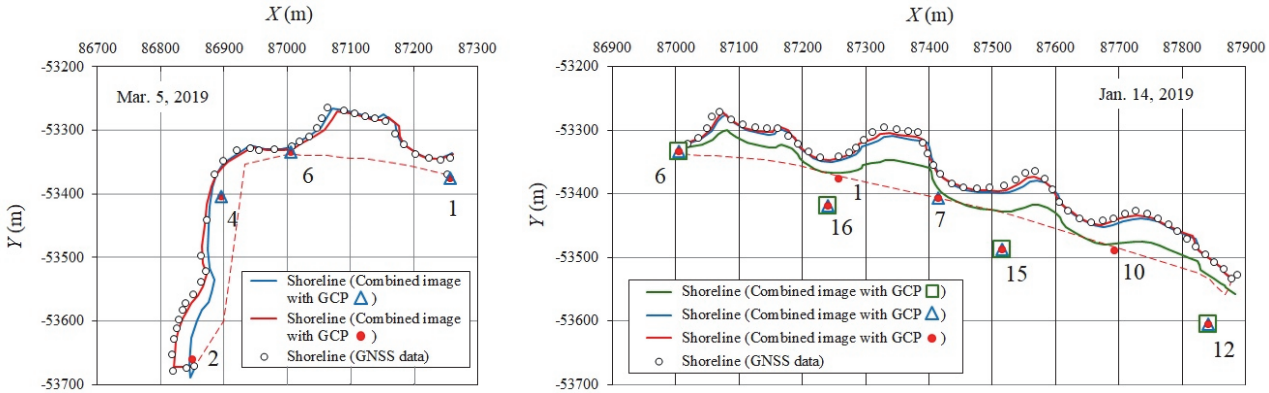

(a) Yuragawa river-mouth zone (b) Kanzaki coastal zone

Figure 7. Effects of GCP on accuracy of estimation results of shoreline.

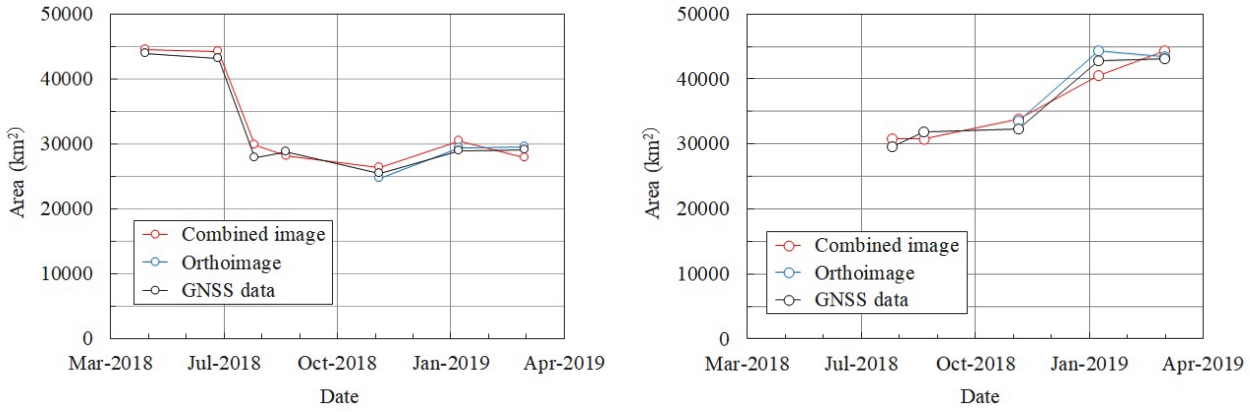

(a) Yuragawa river-mouth zone (b) Kanzaki coastal zone

Figure 8. Estimation results of areas in their temporal variations.

2018) for both zones were used as the GCP. Since the orthoimage contains these two zones, the GCP can be chosen in common. The estimation of the shoreline of Kanzaki coastal zone gives high accuracy compared with the method by using the combined images.

The effects of the selection of GCP on the estimation of shoreline are described in Figure 7. Figure 7(a) shows the effect of GCP No.2 which is located at the southern edge in all GCPs in the zone. That is, when the number of GCP is only three of No.1, 4 and 6, the estimation result of shoreline around No.2 shifts in the East direction from the shoreline measured by the RTK-GNSS survey. This problem is reduced by addition of GCP No.2. Figure 7(b) shows the effect of the location and number of GCP on the estimation of the shoreline. The shoreline colored in green was estimated by using four GCPs of Nos.6, 12, 15 and 16, it is away from the shoreline measured by the RTK-GNSS survey. The reason is that these GCPs are chosen in linear position and parallel direction to the shoreline. The blue line was estimated by using additional GCP of No.7, which is located away from the linear position of the other GCPs, it is improved considerably by the addition of the GCP. The more additional GCPs of No.1 and 10 caused the further improvement of the estimation of the shoreline as shown by the red line. As stated above, since the location and number of GCP affect to the estimation of shoreline, the verification of the GCP rearrangements may be necessary when the target zone has changed remarkably.

Figure 8 shows the estimation results of the areas of Yuragawa river-mouth zone and Kanzaki coastal zone in their temporal variations by using the combined images. The measured results by means of RTK-GNSS survey and the estimation results of them by using the orthoimages are also shown in the figure for comparison. As for the Yuragawa river-mouth zone, the estimation results using the combined images can follow the tendency of the temporal variation. In particular, the large decrease in area due to the flood on early July 2018 can be found. The ratio of the estimated area A_C to the measured one by the RTK-GNSS survey A_G is 0.96 - 1.07. The estimation results of the Kanzaki coastal zone can also follow the tendency of the temporal variation in the area, and the precision accuracy is the same level as the Yuragawa river-mouth zone. The increase in area on November 2018 to January 2019 was based on the accumulation of drift sand in the west area of the zone, whereas its cause is unknown so far. The value of A_C/A_G is 0.95 - 1.05 in this case. These results indicate that since the estimation of areas by means of the combined images and the affine coordinate transformation give a few percent error, the small-scale variations in areas may not be grasped. However, a relatively large-scale variations in areas due to a flood and high wave events can be grasped. On the other hand, the estimation results by using the orthoimage give a high accuracy and precision. The value of A_C/A_G is 0.97 - 1.02 for the Yuragawa

zone and 1.01 - 1.04 for the Kanzaki zone. The sediment contribution to the estuary is from the river in the summer and rainy season and from the ocean in the winter season.

4. CONCLUSIONS

The results obtained in this study are summarized as follows:

1. The area of the river-mouth bar of the Yuragawa River kept on fluctuating until 2018, whereas the fluctuation is not so large after that. That is, the area increased related to the sea wave height in the winter seasons, and it decreased due to floods in rainy and summer seasons. Most of the river-mouth bar has almost been flushed out by some floods in recent years, whereas the expansion of the bar has been identified. This may be because the drift sand from the offshore has more easily entered to the estuary.

2. We proposed the method of calculating coordinate values of stations on lands by using a coordinate transformation using aerial photography images and grand control points (GCPs). The *DRMS* values concerning with the coordinate values of GCPs and their calculated results were approximately 2 to 4 meters for using the combined images, whereas those were approximately 0.3 to 0.6 meters for using the orthoimages. The low accuracy for the combined images may be caused by the distortion of the image and the personal attributes, a certain degree of accuracy could be secured if the selection of the still-image and combination of them are reasonably.

3. The shorelines of the Yuragawa river-mouth zone and the Kanzaki coastal zone can be estimate by the proposed method using the combined aerial images of these zones. However, the reproducibility of the estimation results depends on not only the distortion of the image and the personal attributes but also the unbalanced arrangement of GCP. That is, the GCP for the estimation analysis of the shoreline needs to be arranged dispersively. In particular, since the coastal zone widely extends in one direction, the GCP in the onshore or offshore direction are also required.

4. The temporal variations in the areas of the Yuragawa river-mouth zone and Kanzaki coastal zone could be estimated by the affine coordinate transformation and using the combined aerial images within the error of 5-7%. In this way, since the estimation of areas by the proposed method keep an error within a few percent, the small-scale variations in areas may not be grasped. However, a relatively large-scale variations in areas due to a large flood could also be grasped.

ACKNOWLEDGMENTS

Generation works of orthoimages using Pix4Dmapper were supported by Prof. Masamitsu Kuroiwa and Mr. Shinji Yamamoto, who is technical stuff, Coastal Engineering Laboratory of Tottori University. The authors gratefully acknowledge to their support.

REFERENCES

Fujimaki, H. (2011). Subdivision of Irrigation and Drainage in Drylands. Retrieved January 31, 2020 from http://www.alrc.tottori-u.ac.jp/fujimaki/.

Google. (2018). Google Map. Retrieved September 30, 2018 from https://www.google.com/maps/.

Kanda, K., Miwa, H. and Kato, Y. (2012). Study on dynamic status of river-mouth topography and its control methods in Yuragawa River. *Research report on the Grant-in-Aid for Technical Research Development of River and Erosion-control Technology*, MLIT (in Japanese).

Kawaguchi, S., Suzuki, K., Tsuruta, N. and Asahi, S. (2019). Examination of accuracy of photogrammetry of coastal area by UAV. *Technical note of the Port and Airport Research Institute*, No.1360, 1-24 (in Japanese).

Miwa, H., Kanda, K., Ochi, T. and Kawaguchi, H. (2016). Dynamic state of river-mouth bar in the Yuragawa River and its control under flood flow conditions. *Proc. of the 13rd International Symposium on River Sedimentation*, 710-718.

Kuroiwa, M., Sueyoshi, R., Ichimura, Y. and Fukuoka, K. (2016). Study on Topographic change analysis utilizing UAV. *Journal of JSCE*, Ser.B3 (Ocean Engineering), Vol.72, No.2, I_784-I_789 (in Japanese).

Ministry of Land, Infrastructure, Transport and Tourism. (2020). "i-Construction" web site. Retrieved May 19, 2020 from https://www.mlit.go.jp/tec/i-construction/index.html

Ochi, T., Kanda, K., Miwa, H., Koshi, R. and Nakamura, N. (2015). Dynamic State of river-mouth bar and its control in the Yuragawa River. *Journal of JSCE*, Ser.B1 (Hydraulic Engineering), Vol.71, No.4, I_907-I_912 (in Japanese).

Obanawa, H., Hayakawa, Y., Saito, H. and Gomez, C. (2014). Comparison of DSMs derived from UAV-SfM method and terrestrial laser scanning. *Journal of the Japan Society of Photogrammetry and Remote Sensing*, Vol.53, No.2, 68-74 (in Japanese).

Nakamura, N., Asakura, M., Kanda, K., Miwa, H. and Hosoyamada, T. (2015). Field and numerical studies for formation of sand bar at the Yura River mouth. *Journal of JSCE*, Ser.B1 (Hydraulic Engineering), Vol.71, No.4, I_709-I_714 (in Japanese).

Tanaka, R., Okabayashi, T., Toyama, I. and Yamamoto, K. (2016). A proposal of topographical survey by using motion video taken form drone. *Proceedings of the 8th Symposium on Sediment-Related Disasters*, 61-66 (in Japanese).